STEM CELLS TRANSLATIONAL MEDICINE®

FETAL AND NEONATAL STEM CELLS

Characterization and Angiogenic Potential of Human Neonatal and Infant Thymus Mesenchymal Stromal Cells

SHUYUN WANG,[a] LAKSHMI MUNDADA,[a] SEAN JOHNSON,[a] JOSHUA WONG,[b] RUSSELL WITT,[c] RICHARD G. OHYE,[a] MING-SING SI[a]

Key Words. Thymus gland • Mesenchymal stromal cells • Cardiac surgery • Neonatal • Angiogenesis

[a]Department of Cardiac Surgery, Section of Pediatric Cardiovascular Surgery and [b]Department of Pediatric Cardiology, University of Michigan, Ann Arbor, Michigan, USA; [c]Department of General Surgery, Brigham and Women's Hospital, Boston, Massachusetts, USA

Correspondence: Ming-Sing Si, M.D., 11-735 C.S. Mott Children's Hospital, 1540 East Hospital Drive, Ann Arbor, Michigan 48109-5204, USA. Telephone: 734-936-4978; E-Mail: mingsing@umich.edu

Received October 22, 2014; accepted for publication January 22, 2015; published Online First on February 23, 2015.

1066-5099/2015/$20.00/0

http://dx.doi.org/10.5966/sctm.2014-0240

ABSTRACT

Resident mesenchymal stromal cells (MSCs) are involved in angiogenesis during thymus regeneration. We have previously shown that MSCs can be isolated from enzymatically digested human neonatal and infant thymus tissue that is normally discarded during pediatric cardiac surgical procedures. In this paper, we demonstrate that thymus MSCs can also be isolated by explant culture of discarded thymus tissue and that these cells share many of the characteristics of bone marrow MSCs. Human neonatal thymus MSCs are clonogenic, demonstrate exponential growth in nearly 30 population doublings, have a characteristic surface marker profile, and express pluripotency genes. Furthermore, thymus MSCs have potent proangiogenic behavior in vitro with sprout formation and angiogenic growth factor production. Thymus MSCs promote neoangiogenesis and cooperate with endothelial cells to form functional human blood vessels in vivo. These characteristics make thymus MSCs a potential candidate for use as an angiogenic cell therapeutic agent and for vascularizing engineered tissues in vitro.
STEM CELLS TRANSLATIONAL MEDICINE *2015;4:339–350*

INTRODUCTION

Mesenchymal stromal cells (MSCs) isolated from bone marrow, a tissue with regenerative abilities [1, 2], are being evaluated for degenerative and acquired diseases of tissues and organs (e.g., the heart) that may have relatively limited intrinsic regenerative potential [3]. The human thymus is a vascularized organ that plays a pivotal role in T-lymphocyte development, and its durability in providing a robust acquired immune response throughout the lifespan may be partially attributed to its ability to regenerate after injury, infection, or partial surgical resection. A brisk angiogenic phase that involves the participation of MSCs supports thymus regeneration [4, 5]. The in vivo regenerative and proangiogenic function of resident MSCs in the thymus makes them a potential candidate as a cell therapeutic agent in ischemic diseases of other tissues.

According to the Society of Thoracic Surgeons National Database, severe congenital heart disease requiring surgical correction in the neonatal and infant period occurs in >10,000 patients each year in the U.S. Partial or subtotal thymus resection is required to expose the heart and great vessels during many of these surgical procedures. We and others have identified this normally discarded tissue as a plentiful source of MSCs obtained by enzymatic digestion [6, 7]. However, the use of dissociative enzymes and subsequent washes are significant additional steps for clinical translation of these MSCs into patients and may yield numerous other thymus cell types, such as thymic epithelial cells.

The objective of this investigation was twofold. First, we characterized MSCs isolated by explant culture of mechanically fragmented human neonatal and infant thymus tissue. Second, we investigated the in vitro and in vivo proangiogenic qualities of explant culture-isolated human neonatal thymus MSCs. Our results indicate that discarded human neonatal thymus tissue is a source of MSCs with angiogenic potential.

MATERIALS AND METHODS

Cell Isolation and Culture

All studies were performed under an approved protocol from the University of Michigan institutional review board. After informed consent was given by the parents, discarded thymus tissue from infant heart operations was mechanically minced and subjected to explant culture. Experimental details are shown in the supplemental online data. Unless specified otherwise, all experiments were performed with cells from passages 3–9.

Thymus MSC Isolation Yield Estimate

Thymus tissue fragments from 4 patients were weighed and placed in 35-mm tissue culture dishes for explant culture (3–4 fragments per patient). After 10 days of culture, tissue fragments were removed, and the number of cells in each dish was counted. The average number of cells per gram of tissue was then calculated.

CFU-F Efficiency and Limiting Dilution Assay

All colony-forming unit (CFU) assays were performed with passage 7 thymus MSCs from 8 patients. Experimental details of CFU efficiency (CFE) determination are shown in the supplemental online data. Colonies with $>$50 cells were counted and recorded.

Fibroblastic CFU (CFU-F) prevalence was also estimated by a limiting dilution assay (LDA) [8]. Experimental details are shown in the supplemental online data. CFU-F frequency was then calculated using L-Calc software (Stemcell Technologies, Vancouver, BC, Canada, http://www.stemcell.com).

Thymus MSC Growth Kinetics

Growth kinetics of thymus MSCs isolated from four patients were studied with a cumulative population-doubling analysis. Experimental details are shown in the supplemental online data.

Flow Cytometric Analysis

Surface markers of passage 4–9 thymus MSCs isolated from 6 patients were characterized by flow cytometry using antibodies against CD29, CD44, CD45, CD90, CD105, CD73, CD166, CD49e, CD56, STRO-1, CD271, SSEA-4, HLA-ABC, HLA-DR, and nestin. Experimental details are shown in the supplemental online data.

Pluripotency Gene Expression Analysis

Expression of pluripotency-related genes *Oct-4*, *Sox-2,* and *Nanog* was determined in thymus MSCs (passage 5 or 6, $n = 5$) relative to human induced pluripotent stem cells using quantitative polymerase chain reaction (qPCR). Experimental details are shown in the supplemental online data.

Multilineage Differentiation

The ability of thymus MSCs isolated from three patients to differentiate into osteogenic, adipogenic, and chondrogenic lineages when cultured in specific differentiation media was investigated. Experimental details are shown in the supplemental online data.

CD248 Expression

Expression of CD248 (endosialin) on neonatal human thymus MSCs was performed by immunofluorescent staining. Experimental details are shown in the supplemental online data.

Two-Dimensional Angiogenesis Assay

A two-dimensional (2D) in vitro assay was performed to investigate whether thymus MSCs, with or without human umbilical vein endothelial cells (HUVECs), induced tube formation. Experimental details are shown in the supplemental online data.

Multicellular Spheroid Generation

HUVEC, thymus MSC, and HUVEC plus thymus MSC spheroids used in the three-dimensional (3D) angiogenesis assay and in vivo experiments were created by hanging drop culture. Experimental details are shown in the supplemental online data.

Fluorescent Labeling of Cells and Spheroid Sprouting Time Course Study

HUVECs and thymus MSCs were labeled with the vital cell dyes PKH26 and PKH67, respectively, according to the manufacturer's directions (Sigma-Aldrich, St. Louis, MO, https://www.sigmaaldrich.com). Nuclei were stained with Hoechst 33342 (Molecular Probes, Life Technologies; Thermo Fisher Scientific, Waltham, MA, http://www.thermofisher.com/en/home.html). After completion of the labeling, spheroids were generated as described above and imaged consecutively at 0, 24, and 48 hours after placement in fibrin hydrogel with a confocal microscope. Independent experiments were performed in triplicate.

3D Angiogenesis Assay

Fibrin hydrogel was generated in each well of a 24-well plate, as described, followed by the addition of 75 spheroids per well prior to polymerization to ensure that spheroids were embedded within the hydrogel. There were three spheroid groups: HUVECs, HUVECs plus thymus MSCs, and thymus MSCs. After fibrinogen polymerization, basal EGM-2 was added to each well. Spheroids were then incubated overnight and imaged at $\times$100 using an inverted phase contrast microscope (20 spheroids per group). Images were digitally acquired and then analyzed using NeuronJ plugin (Erik Meijering, http://www.imagescience.org/meijering/software/neuronj/) for ImageJ software (NIH, Bethesda, MD, http://imagej.nih.gov/ij/). Primary sprouts emanating from each spheroid were measured by tracing from the base to the furthest tip. Branches from primary sprouts were measured from their origin to the tip. Cumulative branch length and total number of branches were then calculated for each spheroid. Spheroids located along the edge of the wells or in close proximity to each other were excluded from image analysis. Independent experiments were performed in triplicate. In separate experiments, we explored the effects of modifying the ratio of cell types in combination cell spheroids with thymus MSC/HUVEC ratios of 1:3, 1:1, and 3:1 on spheroid sprouting.

Angiogenic Gene Expression Analysis

To gain insight into the findings demonstrated by the spheroid and monolayer sprouting assays, we evaluated differential gene expression for *VEGFA*, *bFGF*, and *HIF-1α* in the different groups and culture conditions using qPCR. After 48 hours, fibrin gels containing spheroids or cell monolayers were digested with nattokinase (50 fibrinolytic units per milliliter, NSK-SD; Japan Bio Science Laboratory Co., Ltd, Osaka, Japan, http://jbsl-net.com/english/index.html) [9] prior to RNA isolation and qPCR. The effects of modifying the ratio of cell types in combination cell spheroids with thymus MSC/HUVEC ratios of 1:3, 1:1, and 3:1 on angiogenic gene expression were also investigated. Experimental details are shown in the supplemental online data and supplemental online Table 1.

Enzyme-Linked Immunosorbent Assay

Vasculogenic and angiogenic growth factor (VEGFA and bFGF) levels in supernatants were measured using enzyme-linked immunosorbent assay kits (VEGFA kit: Invitrogen, Life Technologies, Thermo Fisher Scientific; bFGF kit: Abcam, Cambridge, MA, http://www.abcam.com), according to the manufacturer's directions. To investigate the effects of the combinations of HUVECs and thymus MSCs on growth factor production, HUVEC, thymus MSC, and HUVEC plus thymus MSC spheroids were generated and embedded in fibrin gel in a 12-well plate (500 spheroids per well), and supernatants were collected after 48 hours of culture for analysis. Independent experiments were performed in triplicate.

In Vivo Assessment of Thymus MSC-Induced Angiogenesis

The care of animals was in accordance with institutional guidelines. Constructs (3 per group) containing 500 spheroids (HUVECs, thymus MSCs, and HUVECs plus thymus MSCs) or no spheroids (control group) were made in 96-well plates with 200 μl of fibrin hydrogel and then were implanted subcutaneously in the dorsal region of NOD/SCID mice (Charles River Laboratories International, Wilmington, MA, http://www.criver.com). Constructs were explanted 14 days after implantation, fixed with 4% paraformaldehyde, serially dehydrated in ethanol solutions, infiltrated with xylene, and then embedded in paraffin. Paraffin blocks were sectioned at 5-μm thickness, mounted on glass slides, and then stained with hematoxylin and eosin. The vessel density within and adjacent to the constructs (between the panniculus carnosus muscle layer and the superficial aspect of the construct) was determined. Details on vessel density quantification are shown in the supplemental online data. To determine the origin of blood vessels identified within and adjacent to the construct, immunohistochemical analysis was performed using a monoclonal antibody specific for human CD31 (Dako, Carpinteria, CA, http://www.dako.com) along with the appropriate secondary antibodies. Cell nuclei were counterstained with hematoxylin. To determine the possibility of natural killer (NK) cell involvement in the observed angiogenesis surrounding and within the construct, a separate group of HUVEC plus thymus MSC constructs were explanted on day 7 (when early infiltrate would have been expected) and evaluated for CD335 (BioLegend, San Diego, CA, http://www.biolegend.com), a NK cell marker.

Statistical Analysis

Data were expressed as mean $\pm$ SD. Statistical differences between multiple groups were determined using one-way analysis of variance (ANOVA) with post hoc Tukey honestly significant difference test. Two-way ANOVA with post hoc Tukey honestly significant difference test was used to analyze angiogenic gene expression and vessel density data. Significance was defined as a p value $<.05$.

RESULTS

Characterization of Explant Culture Isolated Neonatal Human Thymus MSCs

Thymus MSCs were isolated from 10 different neonates and infants (aged 2–150 days; mean age: 51 $\pm$ 61 days) who carried a diagnosis of hypoplastic left heart syndrome, D-transposition of the great arteries, pulmonary atresia, complete atrioventricular septal defect, aortic arch hypoplasia, tetralogy of Fallot, and pulmonary artery sling by using an explant culture method. Only thymus MSCs from patients with an absence of known chromosomal abnormalities (n = 8) were evaluated. Discarded thymus tissue was mechanically minced under sterile conditions in the operating room (Fig. 1A, 1B). After 5–10 days of culture, elongated cells with fibroblastic morphology migrated from thymus tissue onto the culture surface (Fig. 1C). An average of $(1.95 \times 10^5) \pm (2.71 \times 10^5)$ plastic-adherent cells with MSC morphology per gram of thymus tissue was isolated by using this explant culture method (n = 4).

Clonogenicity of thymus MSCs (all between passages 4–9) was evaluated by CFE and CFU-F frequency by limiting dilution assays. Two weeks after plating thymus MSCs (n = 7), we observed a CFE of 20%–57% (Fig. 1D, 1E). Using the LDA method (n = 9), we found that CFU-F frequency was an average of 1 in 166 (range: 1 in 31 to 1 in 467).

We evaluated the growth kinetics of thymus MSCs isolated from four patients. Thymus MSCs displayed exponential growth in nearly 30 population doublings (Fig. 1F). Average doubling time for these thymus MSCs during this period was 2.85 $\pm$ 0.54 days.

Human neonatal thymus MSCs from three different patients differentiated into adipogenic, osteogenic and chondrogenic lineages (Fig. 2A–2D). By flow cytometric analysis, human neonatal thymus MSCs from five different patients were nearly all positive for CD44, CD90, CD29, CD105, CD73, and CD166 and negative for CD45, HLA-DR, CD56, STRO-1, SSEA-4, and nestin (Fig. 2E). Approximately 1%–3% of thymus MSCs were also negative for HLA-ABC.

Human MSCs are also known to express pluripotency genes during early passages, and that may contribute to their regenerative abilities [10–13]. We investigated this characteristic in thymus MSCs (n = 5, passage 5 or 6) with qPCR and found that thymus MSCs expressed low levels of *Oct-4, Nanog*, and *Sox-2* gene expression (supplemental online Fig. 1). All lines that were evaluated consistently expressed low levels of *Oct-4*, whereas there was more variability in the expression of *Nanog* and *Sox-2*.

Proangiogenic Characteristics of Thymus MSCs

Because CD248-positive thymus MSCs have been demonstrated to contribute to angiogenesis during murine thymus regeneration [5], we determined whether human thymus MSCs also expressed this surface marker. With immunofluorescence staining, we found that human thymus MSCs (n = 6) were all positive for CD248 (supplemental online Fig. 2).

We evaluated the in vitro proangiogenic characteristics of thymus MSCs combined with HUVECs using a conventional 2D monolayer method and a quantitative 3D spheroid sprouting assay because 3D culture of MSCs has been demonstrated to potentiate their proangiogenic effects and may be more representative of their in vivo behavior [14, 15].

It is well known that HUVECs cultured on Matrigel form a tubule network after overnight culture [16]. We chose to use fibrin hydrogel instead of Matrigel to eliminate the effects of the angiogenic growth factors contained in the latter. We observed that HUVECs cultured on fibrin hydrogel did not manifest any evidence of tubulogenesis at 48 hours of culture (Fig. 3A). Thymus MSCs tended to cluster together and form multicellular masses when cultured on fibrin hydrogel (Fig. 3B). The combination of thymus

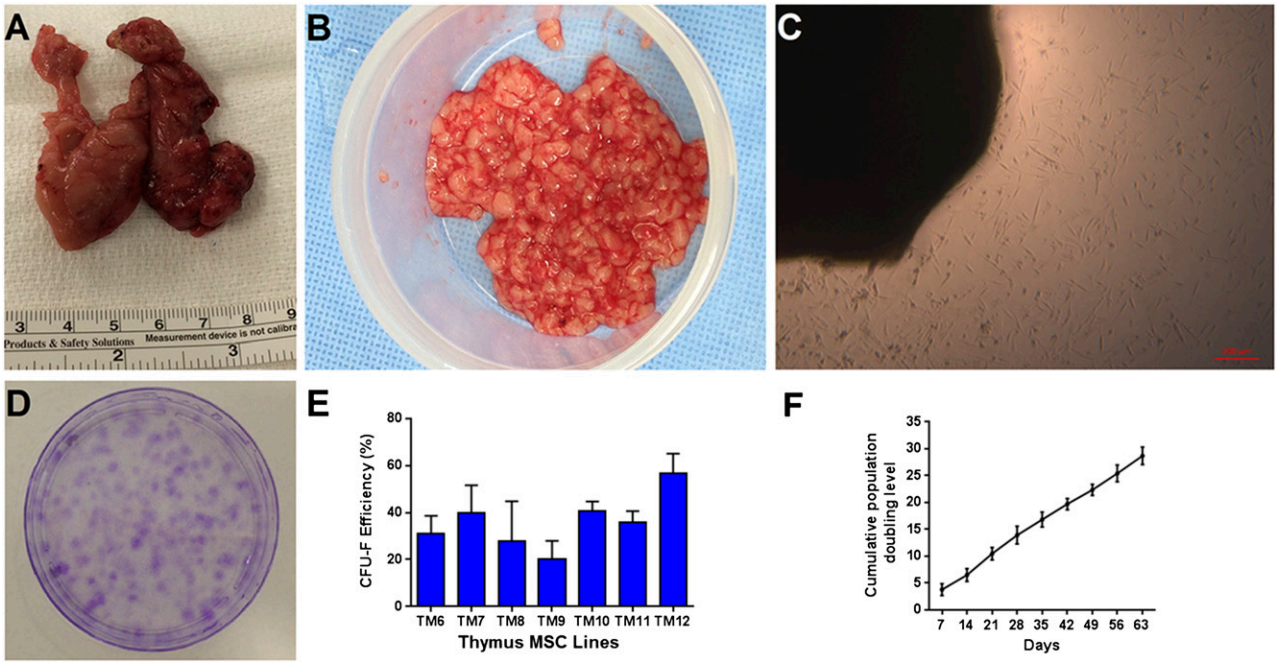

Figure 1. Discarded human neonatal thymus tissue is a source of mesenchymal stromal cells (MSCs). **(A):** Discarded human neonatal thymus tissue during pediatric cardiac surgery. **(B):** Minced thymus tissue prior to plating. **(C):** Cells migrating from thymus tissue fragments during explant culture at 10 days. **(D):** Clonogenicity of thymus MSCs at 2 weeks (representative of 7 donors). **(E):** Colony-forming efficiency of thymus MSCs. **(F):** Averaged cumulative population doubling of thymus MSCs (n = 4) over 9 weeks of culture. Abbreviation: CFU-F, fibroblastic colony-forming unit.

MSCs and HUVECs on fibrin hydrogel yielded an interconnected honeycomb tubule network (Fig. 3C).

Multicellular spheroids embedded in fibrin hydrogel were used for the 3D assessment of angiogenesis. Spheroids composed only of HUVECs did not manifest much sprouting at 16 hours (Fig. 4A). Spheroids composed of only thymus MSCs demonstrated variable sprouting that was dependent on the donor (Figs. 4B–4F). However, spheroids with the combination of HUVECs plus thymus MSCs formed extensive, radiating, tubule-like structures within 16 hours, regardless of donor source of thymus MSCs (Fig. 4G, 4H). The morphology of the sprouts was also distinct in that the combination HUVEC plus thymus MSC spheroids had the most complex branching pattern compared with the thymus MSC-only group (Fig. 4I). At 72 hours, sprouts from HUVEC plus thymus MSC spheroids were more extensive and appeared to anastomose with those from adjacent spheroids (Fig. 4J). We had arbitrarily chosen a 3:1 ratio of HUVECs to thymus MSCs (3:1) because we speculated that endothelial cells (ECs) would outnumber MSCs in vivo based on separate measures of MSCs and ECs in bone marrow [17–19]. We also repeated these sprouting experiments with a HUVEC/thymus MSC ratio of 1:3 and 1:1 and found no significant differences in branch number, and the 1:1 ratio group demonstrated longer total branch length (supplemental online Fig 3).

To understand the contribution of the different cell types to spheroid sprout formation, HUVECs and thymus MSCs were labeled with vital dyes PKH67 and PKH26, respectively. Fluorescent labeling in the combination group of HUVECs plus thymus MSCs revealed that after spheroid formation, MSCs composed the core of the spheroid, whereas the HUVECs remained in the periphery (Fig. 5). After allowing the spheroids to sprout, the thymus MSCs migrated to form the leading edge of the sprouts, whereas the HUVECs composed the core of the spheroid. At 8 hours, many of these sprouts originated from the thymus MSCs, with HUVECs colocalized to a subset of the bases of these sprouts (Fig. 5). At 24 hours, the sprouts had increased in number, complexity, and length. Again, many of the sprouts were composed of thymus MSCs; however, a larger subset also contained HUVECs, which extended further out from the base compared with those observed at the 8-hour time point (Fig. 5).

Thymus MSC Angiogenic Gene and Protein Expression

To gain further insight into the angiogenic sprouting seen in 3D versus 2D culture conditions and the effects of cell composition (HUVECs, thymus MSCs, and HUVECs plus thymus MSCs) on spheroid sprouting, we investigated changes in expression for genes known to play a role in angiogenesis and vasculogenesis: *VEGFA*, *bFGF*, and *HIF-1α*. Culturing HUVECs in spheroids resulted in a decrease in expression of all studied genes compared with monolayer culture. However, placing thymus MSCs in spheroid form had varying effects on the genes (Fig. 6A). For *VEGFA*, expression decreased when thymus MSCs were cultured in spheroids (Fig. 6A). For *bFGF* and *HIF-1α*, expression increased from two to five times when culturing thymus MSCs in spheroid form (Fig. 6A). In monolayer and spheroid culture, thymus MSCs had similar levels of *VEGFA* expression. Relative to thymus MSCs in spheroid form, we noted that combining HUVECs with thymus MSCs resulted in an increase in *VEGFA* expression; however, in this combination of cell types, the expression of *bFGF* or *HIF-1α* did not change or slightly decreased (Fig. 6A). Increasing the thymus MSC content of spheroids resulted in an increase in *VEGFA*, *bFGF*, and *HIF-1α* gene expression (supplemental online Fig 3).

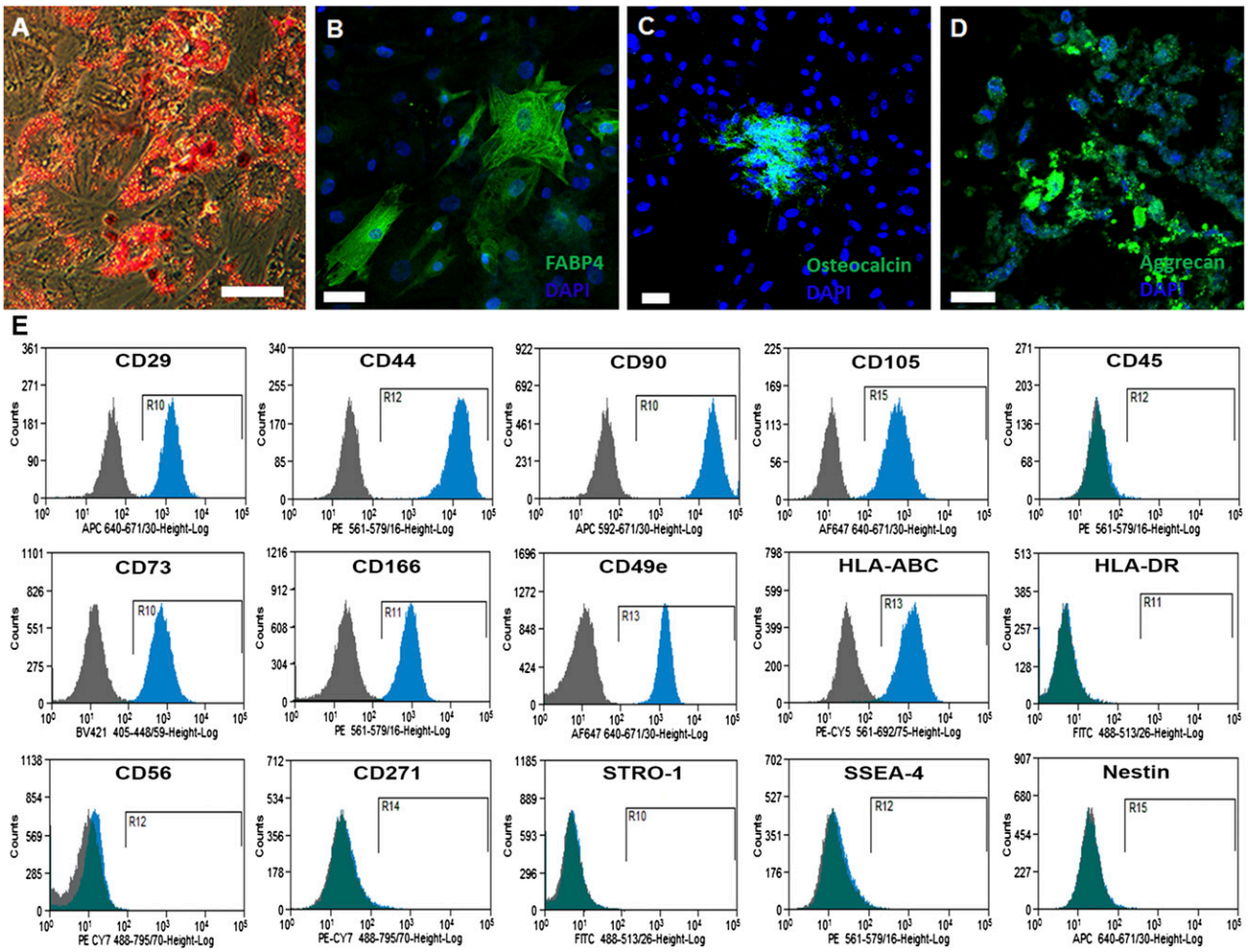

Figure 2. Characterization of human neonatal thymus mesenchymal stromal cells (MSCs) isolated by explant culture. **(A):** Oil Red O staining representing adipogenic differentiation after differentiation with adipogenic-differentiation media. **(B):** FABP-4 expression on thymus MSCs after differentiation with adipogenic-differentiation media. **(C):** Osteocalcin expression on thymus MSCs after differentiation with osteogenic-differentiation media. **(D):** Aggrecan expression on thymus MSCs after differentiation with chondrogenic-differentiation media. All results are representative of three independent experiments. **(E):** Flow cytometric profile of thymus MSCs. All results are representative of thymus MSCs isolated from five to seven patients. Scale bar = 50 μm.

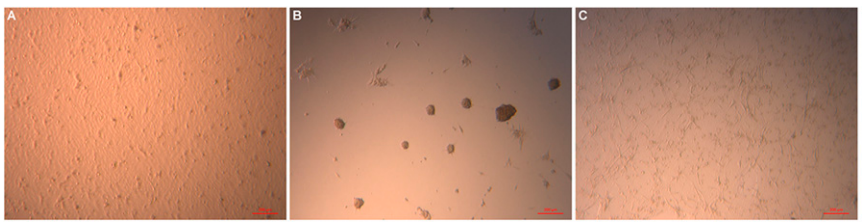

Figure 3. Thymus mesenchymal stromal cells (MSCs) cooperate with human umbilical vein endothelial cells (HUVECs) to form a network in a two-dimensional angiogenesis assay. **(A):** Monolayer appearance of HUVECs after 48 hours of culture on fibrin hydrogel. **(B):** Thymus MSCs clustered together after 24 hours of culture on fibrin hydrogel. **(C):** Combining HUVECs with thymus MSCs (2:1) resulted in the appearance of interconnected tubules at 24 hours. Scale bars = 100 μm. Results are representative of two independent experiments.

Monolayer and spheroid *VEGFA* and *bFGF* gene expression changes were confirmed by measuring protein levels in supernatants (n = 3) (Fig. 6B, 6C). We found that HUVEC spheroids had undetectable VEGFA levels, whereas supernatant VEGFA levels in both thymus MSC spheroids and HUVEC plus thymus MSC spheroids were significantly higher. Supernatant VEGFA levels were not different in HUVEC plus thymus MSC spheroids compared with thymus MSC spheroids (Fig. 6B). Supernatants from HUVEC spheroids contained low levels of bFGF. Thymus MSC spheroids had significantly higher levels of bFGF in the supernatant compared with HUVEC spheroids. The combination of HUVEC plus thymus MSC spheroids yielded the greatest concentration of bFGF in

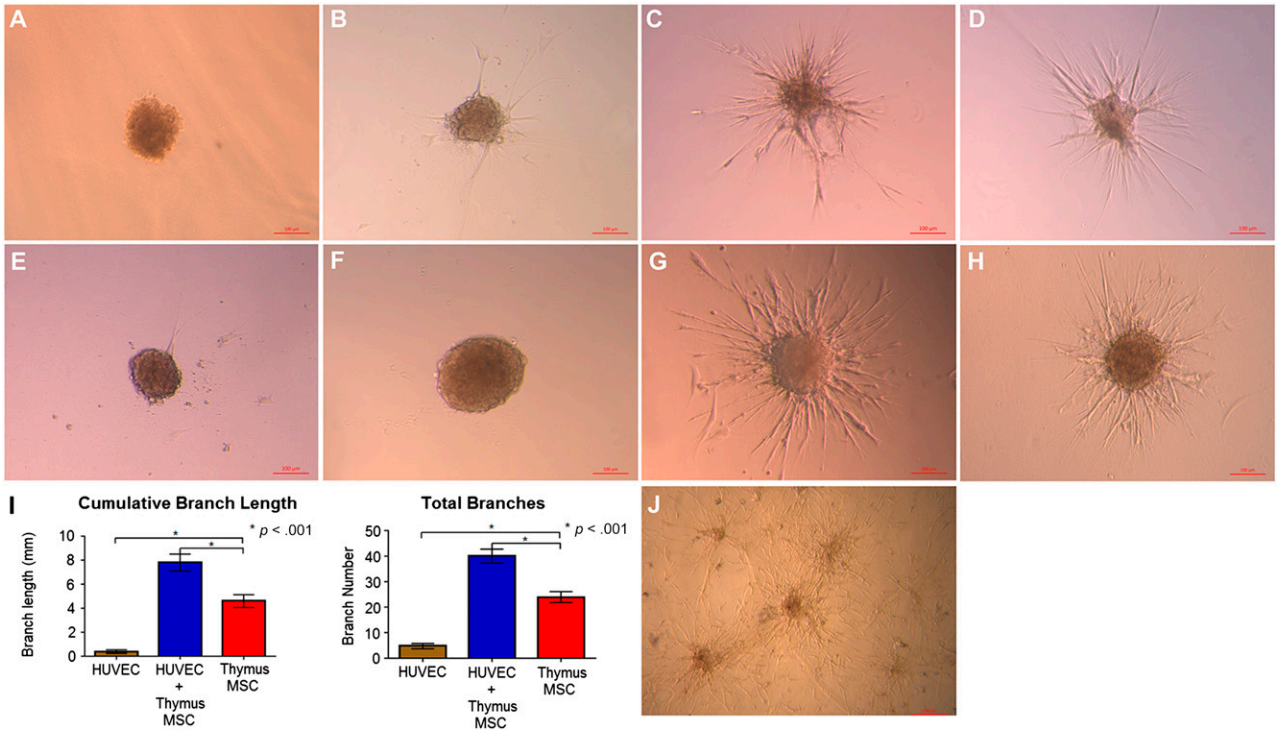

Figure 4. Thymus MSCs cooperate with HUVECs to promote tubule formation in a spheroid three-dimensional (3D) angiogenesis assay. **(A):** Spheroids composed of HUVECs and embedded in fibrin hydrogel did not manifest any sprouting after 16 hours. **(B–F):** Spheroids composed of thymus MSCs isolated from different donors manifested varying degrees of tubule formation at 16 hours. **(G, H):** Spheroids composed of HUVECs plus thymus MSCs (regardless of donor) all demonstrated extensive branching tubule formation at 16 hours. Scale bars = 100 μm. **(I):** Quantitative analysis of 3D angiogenesis assay with HUVEC plus thymus MSC spheroids demonstrating the greatest cumulative branch length and total number of branches (n = 20 spheroids per group). **(J):** Spheroids composed of HUVECs plus thymus MSCs demonstrated complex, anastomosing branches at 72 hours. Results are representative of three independent experiments. Abbreviations: HUVEC, human umbilical vein endothelial cell; MSC, mesenchymal stromal cell.

the supernatant ($p < .05$ vs. supernatants from both HUVEC spheroids and thymus MSC spheroids) (Fig. 6C).

Thymus MSCs Promote In Vivo Vascularization

We evaluated the function of spheroid angiogenic sprouts by implanting fibrin hydrogel constructs containing no cells or spheroids composed of HUVECs, thymus MSCs, and HUVECs plus thymus MSCs subcutaneously in NOD-SCID mice. On explant, control constructs did not appear to manifest any adjacent host reaction, whereas the constructs with spheroids made of thymus MSCs or HUVECs plus thymus MSCs incited an obvious host vascular response (Fig. 7A–7D).

Histologically, controls demonstrated cellular (but avascular) infiltrate from the surrounding tissue. No blood vessels were detectable within the control constructs, and the region adjacent to the construct did not appear to have increased vascularity (Fig. 7E).

Constructs with spheroids from all groups shared several characteristics. First, the central portions of the construct demonstrated "ghosts," or empty pockets, that were indicative of the prior locations of spheroids (Fig. 7F). There were also spheroids within the more interior portions of the constructs that manifested varying degrees of cell death, suggesting that the cells were subjected to ischemia (Fig. 7F). However, spheroids were generally present at the surface of the construct, suggesting that an adequate level of tissue partial pressure of oxygen was present to sustain the survival of these cells. All spheroid groups had an increased cell number and vascularity adjacent to the construct. This increase in vascularity was specifically identified between the panniculus carnosus muscle layer and the more superficial aspect of the construct, whereas no blood vessels were identified deep in the construct (Fig. 7F). This finding suggests that implanted constructs attracted host blood vessels from more superficial (and vascular) regions of the mouse dermis. Any vascularization within a construct occurred at its surface, consistent with the findings of others [20].

Constructs composed of spheroids made of only HUVECs attracted host blood vessels adjacent to the construct but had few vessels penetrate the construct (Fig. 7F). Constructs composed of thymus MSC-only spheroids demonstrated increased cellularity and vascularity surrounding and penetrating these constructs (Fig. 7G). Constructs containing spheroids with both HUVECs and thymus MSCs also demonstrated an increase in adjacent tissue cellularity and vascularity and had the greatest vessel density within the construct (Fig. 7H, 7I). In some regions adjacent to constructs with thymus MSC-only or HUVEC plus thymus MSC spheroids, we noted significant erythrocyte extravasation (data not shown).

To determine the origin of the new blood vessels identified within the constructs, we performed human-specific CD31 staining. We found that only constructs with spheroids containing HUVECs plus thymus MSCs (n = 3) contained human-specific CD31 luminal structures that contained erythrocytes, suggesting

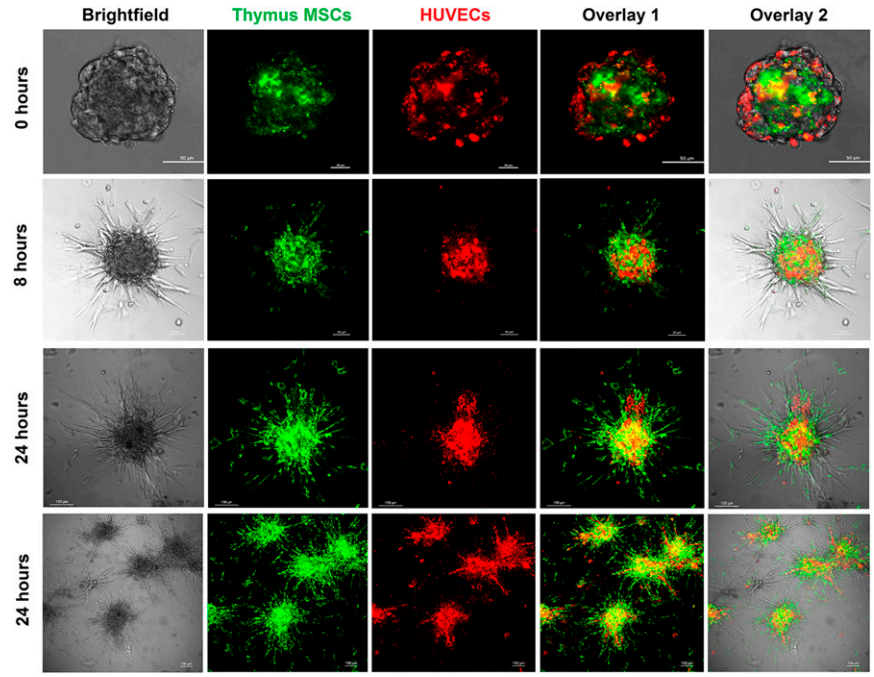

Figure 5. Thymus MSCs initiate the spheroid sprouting response in vitro. HUVECs and thymus MSCs were labeled with PKH26 and PKH67 prior to spheroid formation by overnight hanging drop culture and then embedded in fibrin hydrogel. Spheroids were then imaged with a confocal microscope at the indicated time points. As seen at 0 hour, spheroids with HUVECs and thymus MSCs formed core-shell bodies with MSCs forming the interior core of the spheroid. Spheroids manifested sprouting at 8 hours, with thymus MSCs composing the majority of sprouts and HUVECs colocalized to the bases of a subset of sprouts. At 24 hours, spheroids had more extensive branches, all composed of thymus MSCs and a subset containing HUVECs as well. Scale bars for 0- and 8-hour images = 50 μm. Scale bars for 24-hour images = 100 μm. Results are representative of three independent experiments. Abbreviations: HUVEC, human umbilical vein endothelial cell; MSC, mesenchymal stromal cell.

the formation of functional human vessels that integrated with the host's vasculature (Fig. 7J). Human CD31-positive vessel density from five sections of these HUVEC plus thymus MSC constructs was determined to be 20.9 $\pm$ 10.6 vessels per square millimeter. We did not find any positive CD335 NK cells within or around day 7 explants (supplemental online Fig. 4).

Discussion

One aim of this study was to isolate MSCs from discarded thymus tissue using a nonenzymatic, explant culture technique. Digestive enzymes may damage and/or alter cells and complicate the generation of a cell therapeutic product under good manufacturing practice conditions [21, 22]. Similar to our approach in this study with discarded thymus tissue, others have described the efficient isolation of adipose stem cells by explant culture of lipoaspirate tissue fragments [23–25]. It was not the purpose of our study to optimize MSC isolation from discarded thymus tissue using a manual fragmentation method, and this may explain the variability in the yield that we observed with different samples. However, compared with published results of the isolation of MSCs from adipose tissue, our method of isolating MSCs from thymus tissue appears to provide a comparable yield [26].

We have extended the prior characterization of MSCs from discarded neonatal human thymus tissue isolated by an enzymatic method [6, 7]. In this study, we demonstrated that explant culture-isolated thymus MSCs share many characteristics with bone marrow-derived MSCs. The prevalence of thymus MSC CFU-Fs is comparable to that determined for bone marrow and adipose tissue MSCs [27, 28]. The average thymus MSC doubling was also comparable to those of MSCs isolated from other tissues [29]. Various types of MSCs have been shown to express pluripotency genes [10–12]. We demonstrated that passage 5 and 6 thymus MSCs exhibited low levels of *Oct-4*, *Nanog*, and *Sox-2* gene expression and were also multipotent. Thymus MSCs shared several surface marker characteristics with bone marrow MSCs but also, like MSCs from other tissues, were distinct in that they lacked some of the markers that have been used to identify a subset of bone marrow MSCs such as STRO-1 [30–32]. Unlike amniotic fluid MSCs, neonatal thymus MSCs did not express SSEA-4 [32].

Organ and tissue regeneration requires growth of new tissue or repair of damaged tissue that contributes relevant, organ-specific, physiological function. The regenerative capacity of human organs varies considerably. Although heart, brain, and kidneys appear to have limited regenerative potential after injury, the preadolescent thymus gland possesses an extraordinary ability to regenerate itself after injury and stress. Fundamental to any significant regenerative response of thick tissues and to the engineering of viable thick tissues is the requirement of angiogenesis and vasculogenesis; therefore, regenerative medicine strategies should include components that boost neovascularization [33–37].

We found that thymus MSCs possess proangiogenic characteristics in vitro and in vivo. Although bone marrow MSCs form a tubule network when cultured on Matrigel [38, 39], thymus MSCs tended to cluster together to form microcellular aggregates on fibrin hydrogel. This different behavior may be attributable to

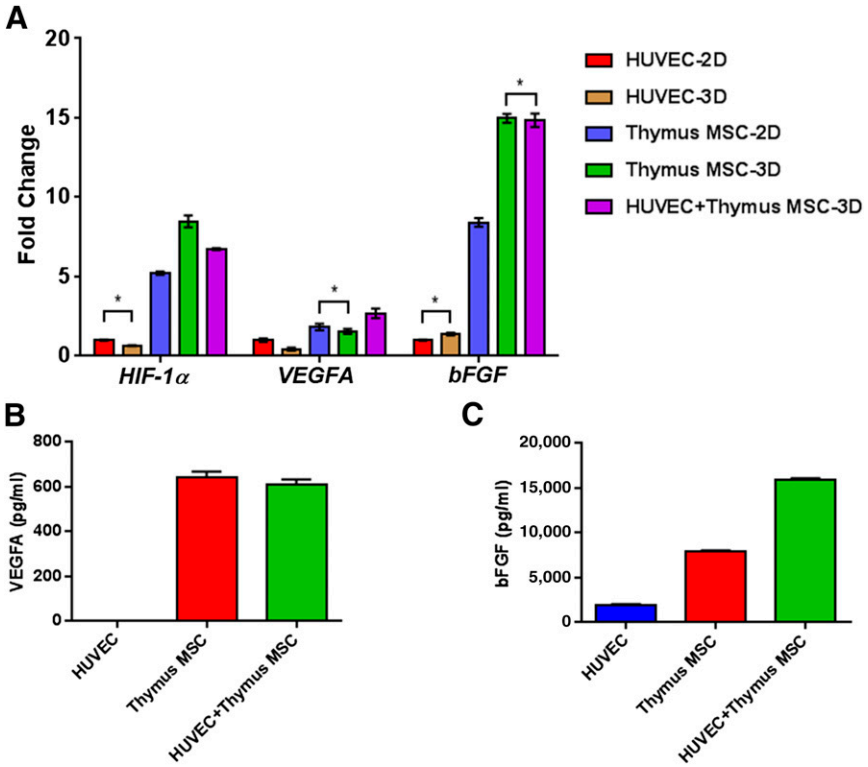

Figure 6. Increased angiogenic gene and protein expression in thymus MSCs. HUVECs and thymus MSCs were cultured as monolayer or in spheroids for 48 hours prior to RNA isolation for quantitative polymerase chain reaction analysis. **(A):** Fold change in expression for *HIF-1α*, *VEGFA*, and *bFGF* relative to HUVECs cultured in spheroids. In general, monolayer and spheroids with thymus MSCs had significantly increased expression of all studied genes. Culturing thymus MSCs in spheroids enhanced the expression of these angiogenic genes. For each gene, all comparisons between groups were significant by two-way analysis of variance (ANOVA) and post hoc Tukey test except those comparisons indicated by an asterisk. **(B, C):** Levels of VEGFA and bFGF in supernatants from spheroid cultures in **(A)** were determined by enzyme-linked immunosorbent assay. VEGFA levels were increased in spheroids containing thymus MSCs, with no apparent effect by culturing with HUVECs. There was no difference in VEGFA levels between thymus MSC and HUVEC plus thymus MSCs groups. In contrast, bFGF levels were significantly higher in spheroids containing both HUVECs and thymus MSCs. Results are representative of three independent experiments. Comparisons were performed by one-way ANOVA with post hoc Tukey test. Abbreviations: 2D, two-dimensional; 3D, three-dimensional; HUVEC, human umbilical vein endothelial cell; MSC, mesenchymal stromal cell.

the composition and biomechanical properties of the fibrin hydrogel [40]. When HUVECs and thymus MSCs were cultured together, a honeycomb tubule network rapidly developed on fibrin hydrogel, suggesting that the addition of HUVECs altered the clustering and contractile behavior of the thymus MSCs.

We also evaluated the angiogenic characteristics of thymus MSCs using an established 3D sprouting assay [41–43] because 3D culture is known to enhance the regenerative abilities of MSCs and more closely approximates the in vivo setting [44–47]. In multicellular spheroids, HUVECs and thymus MSCs are in a 3D, high-cell-density aggregate during initial formation, facilitating direct contact and paracrine cell interactions. These cell interactions can be homotypic (MSC/MSC and EC/EC) or heterotypic (EC/MSC). Although it is clear that thymus MSC spheroids had widespread upregulation of gene expression because of homotypic interactions, the slightly decreased upregulation in angiogenic gene expression in the combination of HUVEC plus thymus MSC spheroids suggested that HUVECs may temper this response (heterotypic interactions) or that this may be a dilutional effect of the HUVEC mRNA that decreases the thymus MSC mRNA signal during qPCR. The decrease in angiogenic gene expression caused by an increase in the ratio of HUVECs to thymus MSCs in spheroids is consistent with either explanation. Regulation of MSCs by endothelial cells in vasculogenesis and angiogenesis has not been delineated in detail and is an area of needed research.

Lee et al. described large core-shell bodies (5,000 cells per spheroid) composed of HUVECs and bone marrow MSCs, with MSCs forming the core and HUVECs forming the shell [48]. These investigators used a two-step process that took 48 hours to force a core-shell body arrangement, and the sprouting from these spheroids was seen first at day 3 after embedding in Matrigel. Our method used overnight hanging drop culture to generate spheroids that demonstrated long sprouts in fibrin hydrogel within 16 hours. The improved sprouting may have been secondary to the difference in angiogenic properties of thymus versus bone marrow MSCs, and allowing thymus MSCs and HUVECs to comingle with each other may have maximized contact and interactions between both cell populations before they sorted into a core-shell formation. The improved sprouting we observed may also be explained by the differences in surrounding matrix and their biophysical properties, which can affect the sprouting response [40, 49].

Recruited supporting cells stabilize nascent angiogenic sprouts [50–53]. Placing thymus MSCs and HUVECs together in spheroids eliminates the recruitment step, potentially explaining the rapid sprouting observed in the heterotypic cell combination

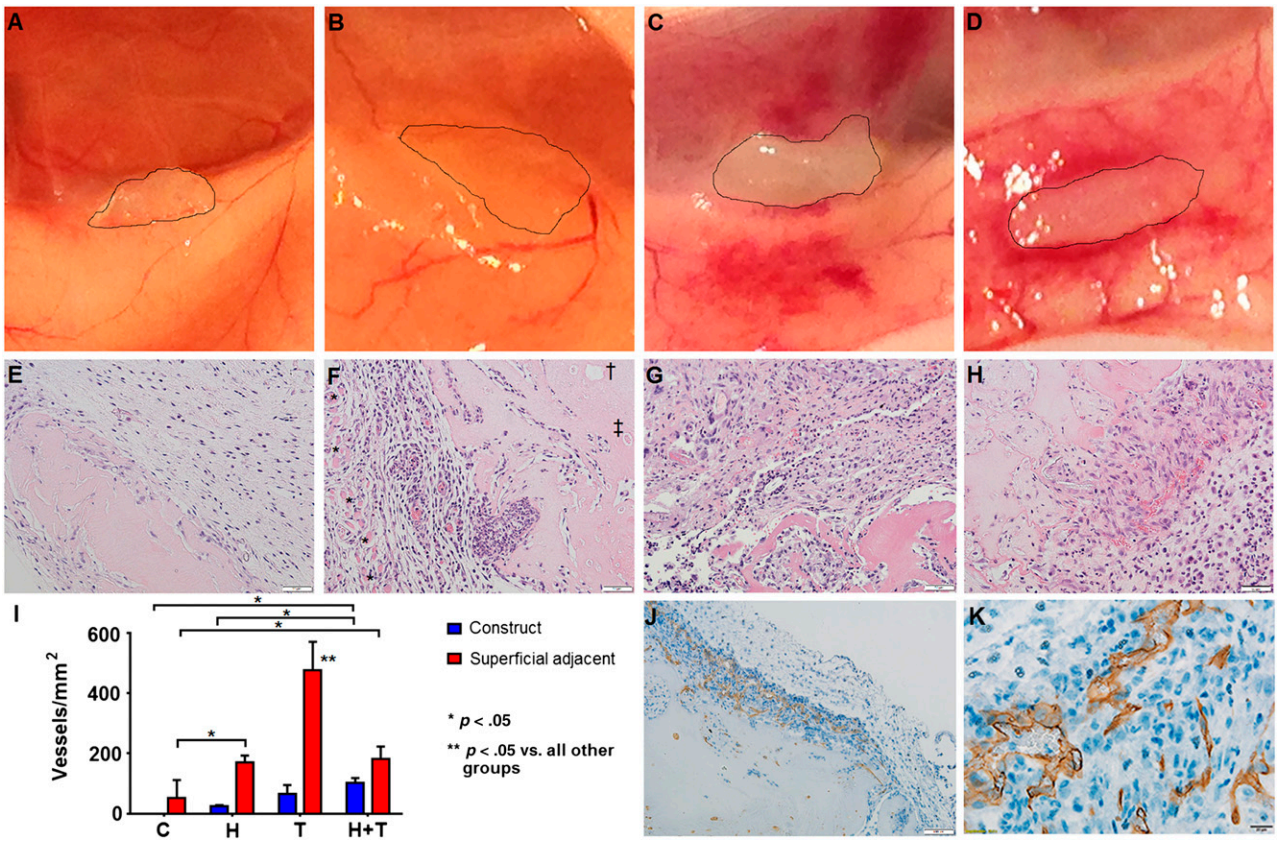

Figure 7. Thymus mesenchymal stromal cells (MSCs) incite angiogenesis in vivo. Fibrin constructs without spheroids (control) or with 500 spheroids with 600 human umbilical vein endothelial cells (HUVECs) per spheroid, 200 thymus MSCs per spheroid, or 600 HUVECs plus 200 thymus MSCs per spheroid were generated (n = 3 per group) and were implanted subcutaneously for 14 days in NOD-SCID mice. Explanted constructs were photographed (edges traced in A–D) and processed for histology. **(A):** Controls did not manifest local reaction. **(B):** HUVEC constructs appeared avascular. **(C):** Thymus MSC constructs were integrated and caused increased adjacent vascularization. **(D):** HUVEC plus thymus MSC constructs were integrated and surrounded by a host vascular response and appeared to have vessels within. **(E–H):** Construct hematoxylin and eosin staining. Scale bars = 50 μm. **(E):** Avascular tissue invasion of control construct. Scale bar = 100 μm. **(F):** HUVEC construct with adjacent cellularity and vascularity between panniculus carnosus muscle layer (*) and construct. "Ghost" (†) of the prior locations of spheroid and necrotic spheroid (‡) were present in internal regions of all constructs with spheroids. **(G):** Thymus MSC construct with increased adjacent cellularity and vascularity. **(H):** HUVEC plus thymus MSC construct with increased vascularization within the construct. **(I):** Manual measurement of vessel density demonstrates significant differences by two-way analysis of variance. Control and HUVEC constructs had minimal adjacent vascularization. Thymus MSC constructs promoted the greatest adjacent response, whereas HUVEC plus thymus MSC constructs contained the greatest vessel density within the construct. **(J, K):** Immunohistochemical staining with human-specific CD31 monoclonal antibody revealed that only constructs with HUVEC plus thymus MSCs contained CD31-positive luminal structures with blood cells. Scale bar = 20 μm. Abbreviations: C, controls; H, human umbilical vein endothelial cell constructs; T, thymus mesenchymal stromal cell construct.

spheroids. It has been speculated that the relative availability of supporting cell-secreted growth factors and their diffusion distance from supporting cells to endothelial cells affects the robustness of tubule formation; therefore, minimizing the distance between endothelial and supporting cell, as in spheroids, may promote microvascularization [49]. In this study, we also found that thymus MSCs may lead the angiogenic sprouting response; this is a new angiogenesis and vasculogenesis paradigm because tip endothelial cells are thought to lead the formation of new sprouts [54–56].

Because of the small diameter of the spheroids that we used, which was well within the oxygen diffusion distance, hypoxia was not expected; however, *HIF-1α* gene expression was upregulated when thymus MSCs were cultured in spheroid form versus monolayer, suggesting a hypoxic response. One possible explanation of this finding is that the oxygen consumption rate for thymus MSCs may be high (or increased during spheroid culture) such that the hypoxia is present at the core of these relatively small spheroids. The combination of thymus MSCs and HUVECs in spheroids demonstrated a decrease in supernatant VEGFA levels. This may represent consumption or binding of VEGFA by HUVECs and/or negative regulation of MSCs by HUVECs and represents an area of future study.

The thymus gland involutes after infection, injury, and chemotherapy [57]. Resolution of thymic stress initiates a potent regenerative response in the thymus gland. Underlying the regenerative potential of the thymus gland is a brisk angiogenic response [4, 5]. This response has been investigated in rodents but has been poorly characterized in humans [4, 5]. Sepsis during the neonatal period has been demonstrated to cause involution [58]. CD248-positive MSCs significantly contributes to the angiogenic response of thymus regeneration in mice [5]. In this study, we demonstrated that thymus MSCs expressed CD248, a cell-surface receptor associated with cell adhesion and migration

[59, 60]. CD248 has also been demonstrated to play a role in peripheral lymph node and splenic expansion and regeneration [61, 62]. The significance of CD248 in the injury and regeneration of other tissues has not been defined, although human bone marrow MSCs, rat adipose MSCs, and blood vessel-associated mural cells express CD248, and an anti-CD248 antibody has been shown to inhibit tube formation in bone marrow MSCs [63, 64].

We found that subcutaneously implanted constructs with homotypic or heterotypic multicellular spheroids attracted host dermal blood vessels, with thymus MSC spheroids inciting the greatest response; however, the combination of HUVECs plus thymus MSCs yielded the greatest vascularization within the construct. This indicates that the cooperation of both cell types promoted the angioinvasion of the adjacent host dermal blood vessels. Furthermore, only the combination of HUVECs plus thymus MSCs yielded the formation of functional human blood vessels, indicating that the importance of the interactions between the two cell types in vasculogenesis. An alternative explanation for the increase in surrounding vascular density is host NK cell-mediated vascular changes because this immune cell is intact in NOD-SCID mice. We performed immunohistochemistry on earlier (day 7) explants to determine the presence of NK cells (CD335) but did not identify any within or around the construct, making NK cell-mediated increase in vascular density less likely.

Although MSCs, with or without endothelial cells, have already been used by others to promote vascularization of implanted constructs and ischemic tissues in both preclinical and clinical settings [47, 65–69], the optimal MSC yielding the maximal therapeutic angiogenic response has yet to be determined. Results presented in this study and elsewhere suggest that thymus MSCs may be a promising candidate for therapeutic use [6, 7]. Given the low expression human leukocyte antigen class I on a subset of neonatal human thymus MSCs, as shown in this study and elsewhere [7, 70], use of these MSCs may also yield advantages in the allogeneic setting (e.g., use in older patients with ischemic heart disease), in which it is more likely to complement the advantages of neonatal MSCs over adult MSCs [71–73]. However, improvements in isolation yield are needed to make clinical use of thymus MSCs feasible.

Other sources of MSCs and stem cells that may have therapeutic potential in neonates with heart disease include amniotic fluid, placenta, umbilical cord, and Wharton's jelly [32, 74–78]. MSCs have also been isolated from aborted fetuses [79]. Similar to human neonatal thymus MSCs, fetal MSCs also had trilineage differentiation capacity. The doubling time for fetal MSCs was slightly less than what we observed in human thymus MSCs, but the CFE was greater in human neonatal thymus MSCs. Like neonatal thymus MSCs, fetal MSCs express pluripotency-related genes such as *Oct-4* and *Nanog* [80, 81]. Full characterization and detailed comparison in relevant disease models are needed to determine which MSC type will yield the optimal therapeutic benefit.

Conclusion

MSCs are present in large numbers in discarded neonatal and infant thymus tissue and can be isolated by an explant culture method. Explant culture-isolated thymus MSCs demonstrate the classical characteristics of bone marrow MSCs. Thymus MSCs also possess proangiogenic qualities and deserve further consideration as a potential cell therapeutic agent to promote tissue regeneration and repair and for use in strategies to vascularize engineered tissues.

Acknowledgments

This work was supported by the University of Michigan, Department of Cardiac Surgery. We thank Kaihong Wu for his technical assistance with cell culture.

Author Contributions

S.W.: conception and design, collection and/or assembly of data, data analysis and interpretation, manuscript writing; L.M.: collection and/or assembly of data, data analysis and interpretation, manuscript writing; S.J.: collection and/or assembly of data; J.W. and R.W.: collection and/or assembly of data, data analysis and interpretation; R.G.O.: provision of study material or patients, manuscript writing, financial support; M.-S.S.: conception and design, provision of study material or patients, collection and/or assembly of data, data analysis and interpretation, manuscript writing, final approval of manuscript.

Disclosure of Potential Conflicts of Interest

The authors indicated no potential conflicts of interest.

References

1 Patt HM, Maloney MA. Bone marrow regeneration after local injury: A review. Exp Hematol 1975;3:135–148.

2 Han W, Yu Y, Liu XY. Local signals in stem cell-based bone marrow regeneration. Cell Res 2006;16:189–195.

3 Georgiou KR, Foster BK, Xian CJ. Damage and recovery of the bone marrow microenvironment induced by cancer chemotherapy - potential regulatory role of chemokine CXCL12/receptor CXCR4 signalling. Curr Mol Med 2010;10:440–453.

4 Park HJ, Kim MN, Kim JG et al. Up-regulation of VEGF expression by NGF that enhances reparative angiogenesis during thymic regeneration in adult rat. Biochim Biophys Acta 2007;1773:1462–1472.

5 Lax S, Ross EA, White A et al. CD248 expression on mesenchymal stromal cells is required for post-natal and infection-dependent thymus remodelling and regeneration. FEBS Open Bio 2012;2:187–190.

6 Sondergaard CS, Hodonsky CJ, Khait L et al. Human thymus mesenchymal stromal cells augment force production in self-organized cardiac tissue. Ann Thorac Surg 2010;90:796–803; discussion 803–804.

7 Siepe M, Thomsen AR, Duerkopp N et al. Human neonatal thymus-derived mesenchymal stromal cells: Characterization, differentiation, and immunomodulatory properties. Tissue Eng Part A 2009;15:1787–1796.

8 Schellenberg A, Hemeda H, Wagner W. Tracking of replicative senescence in mesenchymal stem cells by colony-forming unit frequency. Methods Mol Biol 2013;976:143–154.

9 Carrion B, Janson IA, Kong YP et al. A safe and efficient method to retrieve mesenchymal stem cells from three-dimensional fibrin gels. Tissue Eng Part C Methods 2014;20:252–263.

10 Carelli S, Messaggio F, Canazza A et al. Characteristics and properties of mesenchymal stem cells derived from micro-fragmented adipose tissue. Cell Transplant 2014 [Epub ahead of print].

11 Siegel G, Kluba T, Hermanutz-Klein U et al. Phenotype, donor age and gender affect function of human bone marrow-derived mesenchymal stromal cells. BMC Med 2013;11:146.

12 Tantrawatpan C, Manochantr S, Kheolamai P et al. Pluripotent gene expression in mesenchymal stem cells from human umbilical cord Wharton's jelly and their differentiation potential to neural-like cells. J Med Assoc Thai 2013; 96:1208–1217.

13 Yoon DS, Kim YH, Jung HS et al. Importance of Sox2 in maintenance of cell proliferation and multipotency of mesenchymal stem cells in low-density culture. Cell Prolif 2011; 44:428–440.

14 Bhang SH, Lee S, Shin JY et al. Transplantation of cord blood mesenchymal stem cells as spheroids enhances vascularization. Tissue Eng Part A 2012;18:2138–2147.

15 Skiles ML, Sahai S, Rucker L et al. Use of culture geometry to control hypoxia-induced vascular endothelial growth factor secretion from adipose-derived stem cells: Optimizing a cell-based approach to drive vascular growth. Tissue Eng Part A 2013;19:2330–2338.

16 Ponce ML. Tube formation: An in vitro Matrigel angiogenesis assay. Methods Mol Biol 2009;467:183–188.

17 Méndez-Ferrer S, Michurina TV, Ferraro F et al. Mesenchymal and haematopoietic stem cells form a unique bone marrow niche. Nature 2010;466:829–834.

18 Pittenger MF, Mackay AM, Beck SC et al. Multilineage potential of adult human mesenchymal stem cells. Science 1999;284:143–147.

19 Schweitzer CM, van der Schoot CE, Dräger AM et al. Isolation and culture of human bone marrow endothelial cells. Exp Hematol 1995;23:41–48.

20 White SM, Pittman CR, Hingorani R et al. Implanted cell-dense prevascularized tissues develop functional vasculature that supports reoxygenation after thrombosis. Tissue Eng Part A 2014;20:2316–2328.

21 Dean J, McCarthy D, Golden-Mason L et al. Trephine biopsies are enriched for activated T/NK cells and cytotoxic T cells. Immunol Lett 2005;99:94–102.

22 Carvalho PP, Gimble JM, Dias IR et al. Xenofree enzymatic products for the isolation of human adipose-derived stromal/stem cells. Tissue Eng Part C Methods 2013;19:473–478.

23 Busser H, De Bruyn C, Urbain F et al. Isolation of adipose-derived stromal cells without enzymatic treatment: Expansion, phenotypical, and functional characterization. Stem Cells Dev 2014;23:2390–2400.

24 Priya N, Sarcar S, Majumdar AS et al. Explant culture: A simple, reproducible, efficient and economic technique for isolation of mesenchymal stromal cells from human adipose tissue and lipoaspirate. J Tissue Eng Regen Med 2012; 706–716.

25 Bianchi F, Maioli M, Leonardi E et al. A new nonenzymatic method and device to obtain a fat tissue derivative highly enriched in pericyte-like elements by mild mechanical forces from human lipoaspirates. Cell Transplant 2013;22:2063–2077.

26 Dos-Anjos Vilaboa S, Navarro-Palou M, Llull R. Age influence on stromal vascular fraction cell yield obtained from human lipoaspirates. Cytotherapy 2014;16:1092–1097.

27 Gronthos S, Zannettino ACW. Methods for the purification and characterization of human adipose-derived stem cells. Methods Mol Biol 2011;702:109–120.

28 Dmitrieva RI, Minullina IR, Bilibina AA et al. Bone marrow- and subcutaneous adipose tissue-derived mesenchymal stem cells: Differences and similarities. Cell Cycle 2012;11: 377–383.

29 Banfi A, Muraglia A, Dozin B et al. Proliferation kinetics and differentiation potential of ex vivo expanded human bone marrow stromal cells: Implications for their use in cell therapy. Exp Hematol 2000;28:707–715.

30 Watson JT, Foo T, Wu J et al. CD271 as a marker for mesenchymal stem cells in bone marrow versus umbilical cord blood. Cells Tissues Organs 2013;197:496–504.

31 Roson-Burgo B, Sanchez-Guijo F, Del Cañizo C et al. Transcriptomic portrait of human mesenchymal stromal/stem cells isolated from bone marrow and placenta. BMC Genomics 2014;15:910.

32 Roubelakis MG, Pappa KI, Bitsika V et al. Molecular and proteomic characterization of human mesenchymal stem cells derived from amniotic fluid: Comparison to bone marrow mesenchymal stem cells. Stem Cells Dev 2007;16:931–952.

33 Madeddu P. Therapeutic angiogenesis and vasculogenesis for tissue regeneration. Exp Physiol 2005;90:315–326.

34 Bae H, Puranik AS, Gauvin R et al. Building vascular networks. Sci Transl Med 2012;4: 160ps123.

35 Laschke MW, Harder Y, Amon M et al. Angiogenesis in tissue engineering: Breathing life into constructed tissue substitutes. Tissue Eng 2006;12:2093–2104.

36 Tian L, George SC. Biomaterials to prevascularize engineered tissues. J Cardiovasc Transl Res 2011;4:685–698.

37 Kaully T, Kaufman-Francis K, Lesman A et al. Vascularization—the conduit to viable engineered tissues. Tissue Eng Part B Rev 2009;15:159–169.

38 Malinowski M, Pietraszek K, Perreau C et al. Effect of lumican on the migration of human mesenchymal stem cells and endothelial progenitor cells: Involvement of matrix metalloproteinase-14. PLoS One 2012;7: e50709.

39 Tögel F, Weiss K, Yang Y et al. Vasculotropic, paracrine actions of infused mesenchymal stem cells are important to the recovery from acute kidney injury. Am J Physiol Renal Physiol 2007;292:F1626–F1635.

40 Rao RR, Peterson AW, Ceccarelli J et al. Matrix composition regulates three-dimensional network formation by endothelial cells and mesenchymal stem cells in collagen/fibrin materials. Angiogenesis 2012;15:253–264.

41 Klein D, Weisshardt P, Kleff V et al. Vascular wall-resident CD44+ multipotent stem cells give rise to pericytes and smooth muscle cells and contribute to new vessel maturation. PLoS One 2011;6:e20540.

42 Blacher S, Erpicum C, Lenoir B et al. Cell invasion in the spheroid sprouting assay: A spatial organisation analysis adaptable to cell behaviour. PLoS One 2014;9:e97019.

43 Korff T, Augustin HG. Tensional forces in fibrillar extracellular matrices control directional capillary sprouting. J Cell Sci 1999;112: 3249–3258.

44 Zimmermann JA, McDevitt TC. Preconditioning mesenchymal stromal cell spheroids for immunomodulatory paracrine factor secretion. Cytotherapy 2014;16: 331–345.

45 Alimperti S, Lei P, Wen Y et al. Serum-free spheroid suspension culture maintains mesenchymal stem cell proliferation and differentiation potential. Biotechnol Prog 2014;30: 974–983.

46 Cheng NC, Chen SY, Li JR et al. Short-term spheroid formation enhances the regenerative capacity of adipose-derived stem cells by promoting stemness, angiogenesis, and chemotaxis. Stem Cells Translational Medicine 2013; 2:584–594.

47 Laschke MW, Schank TE, Scheuer C et al. Three-dimensional spheroids of adipose-derived mesenchymal stem cells are potent initiators of blood vessel formation in porous polyurethane scaffolds. Acta Biomater 2013;9: 6876–6884.

48 Lee WY, Tsai HW, Chiang JH et al. Core-shell cell bodies composed of human cbMSCs and HUVECs for functional vasculogenesis. Biomaterials 2011;32:8446–8455.

49 Ghajar CM, Chen X, Harris JW et al. The effect of matrix density on the regulation of 3-D capillary morphogenesis. Biophys J 2008; 94:1930–1941.

50 Bergers G, Song S. The role of pericytes in blood-vessel formation and maintenance. Neuro Oncol 2005;7:452–464.

51 Betsholtz C, Lindblom P, Gerhardt H. Role of pericytes in vascular morphogenesis. EXS 2005;115–125.

52 Stratman AN, Davis MJ, Davis GE. VEGF and FGF prime vascular tube morphogenesis and sprouting directed by hematopoietic stem cell cytokines. Blood 2011;117:3709–3719.

53 Davis GE, Stratman AN, Sacharidou A et al. Molecular basis for endothelial lumen formation and tubulogenesis during vasculogenesis and angiogenic sprouting. Int Rev Cell Mol Biol 2011;288:101–165.

54 Paul JD, Coulombe KL, Toth PT et al. SLIT3-ROBO4 activation promotes vascular network formation in human engineered tissue and angiogenesis in vivo. J Mol Cell Cardiol 2013;64:124–131.

55 Hellström M, Phng LK, Hofmann JJ et al. Dll4 signalling through Notch1 regulates formation of tip cells during angiogenesis. Nature 2007;445:776–780.

56 Suchting S, Freitas C, le Noble F et al. The Notch ligand Delta-like 4 negatively regulates endothelial tip cell formation and vessel branching. Proc Natl Acad Sci USA 2007;104: 3225–3230.

57 Dooley J, Liston A. Molecular control over thymic involution: From cytokines and microRNA to aging and adipose tissue. Eur J Immunol 2012;42:1073–1079.

58 Basu S, Dewangan S, Shukla RC et al. Thymic involution as a predictor of early-onset neonatal sepsis. Paediatr Int Child Health 2012;32: 147–151.

59 Valdez Y, Maia M, Conway EM. CD248: Reviewing its role in health and disease. Curr Drug Targets 2012;13:432–439.

60 Tomkowicz B, Rybinski K, Foley B et al. Interaction of endosialin/TEM1 with extracellular matrix proteins mediates cell adhesion and migration. Proc Natl Acad Sci USA 2007;104: 17965–17970.

61 Lax S, Hardie DL, Wilson A et al. The pericyte and stromal cell marker CD248 (endosialin) is required for efficient lymph node expansion. Eur J Immunol 2010;40:1884–1889.

62 Lax S, Hou TZ, Jenkinson E et al. CD248/endosialin is dynamically expressed on a subset of stromal cells during lymphoid tissue development, splenic remodeling and repair. FEBS Lett 2007;581:3550–3556.

63 Bagley RG, Weber W, Rouleau C et al. Human mesenchymal stem cells from bone marrow express tumor endothelial and stromal markers. Int J Oncol 2009;34:619–627.

64 Christian S, Winkler R, Helfrich I et al. Endosialin (Tem1) is a marker of tumor-associated myofibroblasts and tumor vessel-associated mural cells. Am J Pathol 2008;172: 486–494.

65 Kapur SK, Wang X, Shang H et al. Human adipose stem cells maintain proliferative, synthetic and multipotential properties when suspension cultured as self-assembling spheroids. Biofabrication 2012;4:025004.

66 Lee WY, Wei HJ, Wang JJ et al. Vascularization and restoration of heart function in rat myocardial infarction using transplantation of human cbMSC/HUVEC core-shell bodies. Biomaterials 2012;33:2127–2136.

67 Karantalis V, DiFede DL, Gerstenblith G et al. Autologous mesenchymal stem cells produce concordant improvements in regional function, tissue perfusion, and fibrotic burden when administered to patients undergoing coronary artery bypass grafting: The Prospective Randomized Study of Mesenchymal Stem Cell Therapy in Patients Undergoing Cardiac Surgery (PROMETHEUS) trial. Circ Res 2014;114: 1302–1310.

68 Suncion VY, Ghersin E, Fishman JE et al. Does transendocardial injection of mesenchymal stem cells improve myocardial function locally or globally?: An analysis from the Percutaneous Stem Cell Injection Delivery Effects on Neomyogenesis (POSEIDON) randomized trial. Circ Res 2014;114:1292–1301.

69 Ascheim DD, Gelijns AC, Goldstein D et al. Mesenchymal precursor cells as adjunctive therapy in recipients of contemporary left ventricular assist devices. Circulation 2014;129: 2287–2296.

70 Lee WI, Khim M, Im IR et al. Safe and effective gene transfer by adeno-associated virus of neonatal thymus-derived mesenchymal stromal cells. Tissue Cell 2011;43:108–114.

71 Li Y, Charif N, Mainard D et al. Donor's age dependent proliferation decrease of human bone marrow mesenchymal stem cells is linked to diminished clonogenicity. Biomed Mater Eng 2014;24(suppl):47–52.

72 Zaim M, Karaman S, Cetin G et al. Donor age and long-term culture affect differentiation and proliferation of human bone marrow mesenchymal stem cells. Ann Hematol 2012;91: 1175–1186.

73 Wu W, Niklason L, Steinbacher DM. The effect of age on human adipose-derived stem cells. Plast Reconstr Surg 2013;131:27–37.

74 Corrao S, La Rocca G, Lo Iacono M et al. New frontiers in regenerative medicine in cardiology: The potential of Wharton's jelly mesenchymal stem cells. Curr Stem Cell Res Ther 2013;8:39–45.

75 Weber B, Zeisberger SM, Hoerstrup SP. Prenatally harvested cells for cardiovascular tissue engineering: Fabrication of autologous implants prior to birth. Placenta 2011;32(suppl 4):S316–S319.

76 Malek A, Bersinger NA. Human placental stem cells: Biomedical potential and clinical relevance. J Stem Cells 2011;6:75–92.

77 Pappa KI, Anagnou NP. Novel sources of fetal stem cells: Where do they fit on the developmental continuum? Regen Med 2009;4: 423–433.

78 Cantero Peral S, Burkhart HM, Oommen S et al. Safety and feasibility for pediatric cardiac regeneration using epicardial delivery of autologous umbilical cord blood-derived mononuclear cells established in a porcine model system. STEM CELLS TRANSLATIONAL MEDICINE 2015;4:195–206.

79 Campagnoli C, Roberts IA, Kumar S et al. Identification of mesenchymal stem/progenitor cells in human first-trimester fetal blood, liver, and bone marrow. Blood 2001;98:2396–2402.

80 Brady K, Dickinson SC, Guillot PV et al. Human fetal and adult bone marrow-derived mesenchymal stem cells use different signaling pathways for the initiation of chondrogenesis. Stem Cells Dev 2014;23: 541–554.

81 Guillot PV, Gotherstrom C, Chan J et al. Human first-trimester fetal MSC express pluripotency markers and grow faster and have longer telomeres than adult MSC. STEM CELLS 2007; 25:646–654.

See www.StemCellsTM.com for supporting information available online.